An Adaptive Semi-Autonomous Impedance Controller for Teleoperated Object Grasping Based on Human Grip Safety Margin

Popken, M.H.J.; Prendergast, J.M.; Wiertlewski, M.; Peternel, L.

DOI
10.1109/Humanoids57100.2023.10375144

Publication date
2023

Document Version
Final published version

Published in
Proceedings of the 2023 IEEE-RAS 22nd International Conference on Humanoid Robots (Humanoids)

An Adaptive Semi-autonomous Impedance Controller for Teleoperated Object Grasping based on Human Grip Safety Margin

Marlies Popken, J. Micah Prendergast, Michaël Wiertlewski, and Luka Peternel*

2023 IEEE-RAS 22nd International Conference on Humanoid Robots (Humanoids) | 979-8-3503-0327-8/23/$31.00 ©2023 IEEE | DOI: 10.1109/HUMANOIDS57100.2023.10375144

***Abstract*— Humans can effortlessly grasp various objects when the fingers are in direct physical interaction with the object. However, the same actions become complicated when grasping has to be performed via a teleoperated remote robot due to a lack of direct contact and reduced sensory information. Having a fully autonomous remote robot can eliminate the problem of lack of proper feedback to the human operator, nevertheless, it also prevents human control over the remote robot's grasping actions. In this paper, we propose a semi-autonomous controller for a teleoperated robot grasping where the human operator controls the grasping aperture while the robot controls the impedance of the gripper. When the operator grasps an object with the remote robot, the semi-autonomous controller maintains the grip force by adjusting stiffness. The developed stiffness adjustment approach derives from the concept of grip force safety margin, which is the central regulation principle humans use to maintain a light grasp yet prevent object slippage. To detect incipient slippage, we use a tactile sensor that captures the local deformations due to the contact and interprets them to determine the proximity to the object's slip. To validate the proposed method, we performed experiments on a teleoperation system composed of Force Dimension sigma.7 haptic interface and a KUKA LBR iiwa collaborative robot equipped with a custom-built gripper. The results show that the proposed controller is robust to external perturbations while it adapts to the operator's commands to prevent grasped object slippage.**

I. Introduction

Humanoid robots are capable of performing tasks in hazardous environments or locations humans cannot reach, such as disaster areas [1]. However, humanoid robots still lack the dexterity and the cognitive capabilities of humans to accomplish various tasks independently and human involvement is often still required. Such human involvement can be achieved with teleoperation which enables a human operator to perform a task with a remote robot via multiple degrees of freedom interfaces.

A typical action in teleoperation is object grasping, which is essential for the successful execution of a wide range of manipulation tasks. Humans excel at directly grasping objects. When squeezing and lifting the object, we constantly regulate the grip force based on the sense of touch [2]–[4]. Additionally, humans tend to minimise the impact forces while establishing contact with an object [5]. To maintain grasp stability (i.e., object not slipping from the fingers) after the contact is established, humans apply 10-40% more grip force than the minimum required, which is called the grip force safety margin [2]–[4].

The authors are with Cognitive Robotics, Delft University of Technology, Delft, The Netherlands.

*Corresponding author (e-mail: l.peternel@tudelft.nl).

While humans can easily perform various complex grasping actions when in direct physical interaction with an object, the same actions become complicated when performed via a teleoperated remote robot. In teleoperation, the human operator does not have direct physical contact with the grasped object, which impairs the operator's perception and control of the forces required during manipulation. This can lead to the operator applying too much force and damaging the object, or too little force, causing it to slip and fall. While complex feedback interfaces, such as sensorised hand exoskeletons [6], can replicate the tactile feel at the operator's fingers, they may not fully reproduce the capabilities of humans during direct grasping (especially with time delays in the teleoperation loop and limitations on transparency). Therefore, the remote robot grasp controller is important to help the operator maintain a stable grasp on the remote side.

Generally, teleoperated grasping control methods can be categorised into three groups: position [6], force [7]–[9], hybrid position/force [10] and impedance control [11]–[14]. These control methods have different qualities. A position controller takes the commanded position from the local device as a reference for the remote robot. Since the position controller only cares about reaching the desired position and applies as much force as needed to reach it, it can potentially damage the object if the position commands are inaccurate. For example, if the operator commands the remote gripper to grasp a delicate glass and sets a target position inside it, the resulting high forces could crush the glass. On the other hand, the force controller takes the commanded force from the local device as a reference at the remote gripper. The controller at the remote robot applies the commanded force independently of the gripper's position. While in this case a safe force can be maintained, the operator has no control over the grasp position. This could, for example, prevent shaping deformable objects into a desired shape while being grasped.

While a position controller does not care about the force, and a force controller does not care about the position, the advantage of an impedance controller is that it controls the relation between position and force. For example, when teleoperating a gripper to grasp a cup, the impact force can be reduced if the impedance is set low, while the operator still has control over the position. The operator can also directly control the impedance of the remote robot through teleimpedance [15], employing interfaces based on muscle activity [11], [14] or external devices [16]. However, this requires extra hardware and additional effort from the operator, while reduced sensory information may still be detrimental to achieving grip safety margin in real-time. Several semi-

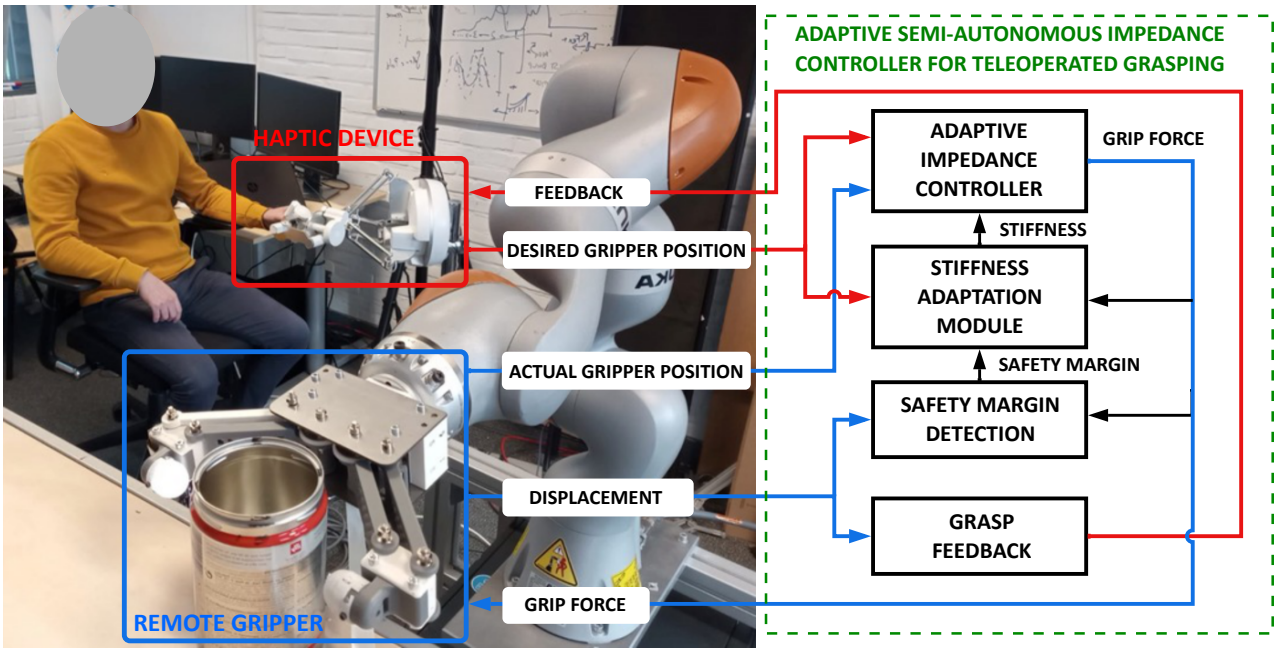

Fig. 1. Overview of the semi-autonomous adaptive impedance controller. On the left is a tele-grasping setup. On the right is a schematic overview of the controller that consists of four parts: adaptive impedance controller, stiffness adaptation module, safety margin detection, and grasp feedback.

autonomous impedance controllers have been proposed to relieve the operator from commanding the impedance to the remote robot so that they can entirely focus on commanding the position [17]–[20]. However, these controllers do not take into account the grip safety margin and may not ensure that the applied grip force guarantees grasp stability.

To address this gap, we propose a semi-autonomous controller for tele-grasping where the operator maintains the ability to command the desired gripper aperture (position), while the autonomous impedance controller ensures grasp stability via a grip safety margin approach. A schematic overview is shown in Fig. 1. This method achieves that 1) the operator controls the aperture (position) of the remote gripper, and 2) the grip force is controlled autonomously to maintain grasp stability. More details about this controller are described in Section II. In summary, the contributions of this paper are:

- A semi-autonomous controller for tele-grasping where the control over the remote gripper is shared between the human operator and the robot to enable the operator to control the gripper aperture while the robot controls the grasp stability through impedance adjustments.
- A critical deformation parameter identification procedure used for grip force safety margin detection that can be performed by the operator online during teleoperation, as an alternative to offline calibration procedures based on a large training dataset.

To test the controller, we implemented it on a tele-grasping setup, which consists of a local haptic device that the operator uses to control a gripper on a remote robotic arm. We performed two proof-of-concept experiments to demonstrate the main functionalities of the proposed method. The experiments *adaptability to external changes* and *adaptability to human input* test the controller during load force changes and operator input perturbations (Section III). The results show that the controller maintains grasp stability (Section IV) and a discussion of the results is given in Section V.

II. Method

The proposed method consists of four elements (Fig. 1): adaptive semi-autonomous impedance controller for grasping (Section II-A), stiffness adaptation module (Section II-B), safety margin detector (Section II-C), and grasp feedback (Section II-D). The adaptive semi-autonomous impedance controller enables the operator to control the aperture (position) of the remote gripper while the robot controls the forces. The force at the remote gripper is regulated by the stiffness adaptation module, which adjusts the stiffness and damping to ensure grasp stability during grasping while maintaining compliance in non-grasped phases of operation. The stiffness adaptation module relies on the safety margin detector to maintain grasp stability. Finally, force feedback is provided to the operator to inform when contact is made with an object.

A. Adaptive impedance controller

While the operator also controls the pose of the robotic arm through the haptic device, the focus of the proposed method is on the control of gripper fingers for grasping. The gripper control is split between the aperture position, which is handled by the operator, and the gripper impedance at the fingers, which is handled by the adaptive semi-autonomous impedance controller. The gripper impedance controller is defined by the impedance control law [21] as

$$F = K(x_r - x_a) + D(\dot{x}_r - \dot{x}_a), \tag{1}$$

where F is the gripper force between the fingers and the object, x_r, is the desired reference gripper aperture position commanded by the operator, x_a the actual gripper aperture position of the remote robot as measured by the encoder, while K and D are Cartesian stiffness and damping terms that define impedance of the fingers and are determined by the stiffness adaptation module. In a general case, F, x_r, and x_a are vectors while K and D are matrices, i.e., when grippers with multiple degrees of freedom (DoF) are employed. In this paper, we used a gripper with one-DoF fingers, thus these variables can be simplified to scalars.

B. Stiffness adaptation module

The main goal of the stiffness adaptation module is to adapt the stiffness and damping terms of the gripper in (1) to the task where a certain object with specific properties is grasped. When the gripper is not grasping or touching an object, the stiffness term is set to a low value defined by parameter K_0, creating a compliant low-impedance controller. This low impedance is useful for establishing safe contact between the fingers and unknown objects in unstructured environments. After the gripper establishes safe contact with an object, i.e., when a small stable force is measured, the stiffness term becomes dependent on the safety margin to enable the adaptive impedance controller to apply a force equivalent to grasp stability. We achieve this by an integral controller that adapts the stiffness based on the error between the reference safety margin and the detected safety margin as

$$K = K_0 + I \int e \, dt, \tag{2}$$

$$e = \Gamma_r - \Gamma, \tag{3}$$

where K_0 the feed-forward term of the controller to make the gripper compliant in case of no contact, I is the gain of the integral controller, Γ the detected safety margin, Γ_r the reference safety margin, and K is the commanded stiffness term calculated based on the last detected safety margin. The damping term D is controlled based on the current stiffness to achieve a critically damped system as $D = 2 \cdot 0.7\sqrt{K}$ [22]. As with (1), K, D, K_0, and I are generally matrices but for grippers with one-DoF fingers they can be simplified to scalars. In the case of multiple DoF, K and D have to be aligned with the direction of the contact with the object, where eigendecomposition or singular value decomposition can be employed to rotate the matrices.

C. Safety margin detection

The proposed adjusting of the gripper stiffness is inspired by the human grasp stability based on a grip force safety margin Γ. Humans typically apply 10-40% more grip force than the minimum required. This can be achieved based on the frictional state of the object, where the safety margin can be viewed as an estimate of how close an object is to slippage [2], [3]. The safety margin can be determined by the minimal required grip force, which depends on the lateral force and the coefficient of friction of the grasped object. There is no slippage as long as static friction is present between the object and the gripper. This is described by a classic expression for static friction as

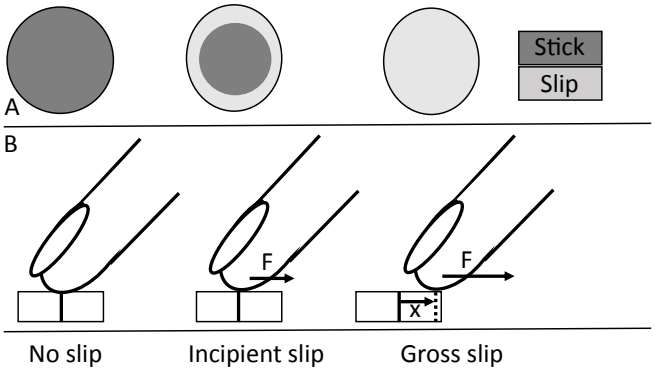

Fig. 2. Stages of slip between a fingertip and an object. **A**) The stick-slip ratio in the contact surface. **B**) The displacement and the force exerted by a fingertip

$$F_l \leq \mu_s F, \tag{4}$$

where F_l is the lateral force, μ_s is the static coefficient of friction, and F is the grip force. An object starts to slip when kinetic friction occurs, which is described by a classic expression for kinetic friction as

$$F_l^* = \mu_k F, \tag{5}$$

where F_l^* is the critical lateral force and μ_k is the kinetic coefficient of friction. The critical lateral force F_l^* is thus the force above which slippage occurs. As long as $F_l < F_l^*$, the object is not slipping. Based on this difference between the lateral force and the critical lateral force, the safety margin Γ can be computed [23]

$$\Gamma = 1 - \frac{F_l}{F_l^*}. \tag{6}$$

Slippage consists of two stages: incipient slip and gross slip (Fig. 2). During incipient slip, the contact area between the gripper and the object deforms and detaches from the object in the peripheral area of the contact surface, causing slippage in the outer area of the contact surface. Despite this, there is no relative movement because the centre of the contact area remains in contact with the object, which can withhold the lateral force. As incipient slip increases, the detachment moves towards the centre of the contact area. When the contact area cannot withhold the lateral force anymore, the entire area detaches and there is relative displacement leading to gross slip.

The approach in (6) requires measured force and typical mechano-electric tactile sensors rely on displacement to measure strain [8], [24], [25]. However, displacement only occurs during the gross slip stage and thus mechano-electric tactile sensors cannot preemptively detect slippage. An alternative method is to compute the safety margin based on deformations in the contact surface between the object and the gripper, which emerge due to indentation, shear stress and slippage. Such deformation can be measured visually with camera-based sensors [26], [27]. Using this information, we

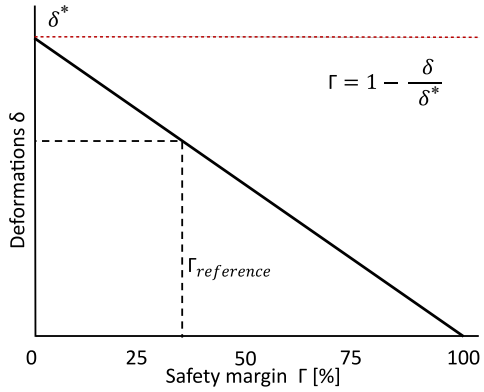

Fig. 3. The safety margin relative to the deformations in the contact area. The critical deformation δ^*, at which gross slip occurs, is represented by the red horizontal line.

can estimate the safety margin already during the incipient slip stage, i.e., before the relative displacement occurs.

We track the deformations in the contact area between the grasped object and the gripper. These deformations are caused by incipient slip and are indicative of how close an object is to gross slippage, which corresponds to the safety margin. This enables us to compute the safety margin Γ as

$$\Gamma = 1 - \frac{\delta}{\delta^*}, \tag{7}$$

where δ and δ^* are the measured and the critical deformation, respectively. The details about how the actual deformation δ is measured are provided in Section III-A. Critical deformation δ^* occurs when the object is on the verge of gross slippage and depends on the grip force and the material of the grasped object. Therefore, every object has a set of critical deformations that correspond to different grip forces.

The safety margin, relative to the deformation in the contact surface, is visualised in Fig. 3. The safety margin is 0 when $\delta = \delta^*$, and the object is on the verge of gross slippage. When $\delta < \delta^*$ the safety margin is between 0 and 100%. The grip force is then adapted through gripper stiffness according to (2)-(3) to fit a deformation that corresponds with the reference safety margin Γ_r. We set $\Gamma_r = 30\%$ to be in the upper middle of the typical human range of 10-40%.

The study in [28] already showed that predicting safety margin based on deformations is possible. The images capturing deformations caused by incipient slip were validated with force measurements and used as an input to neural networks, which predicted safety margin as an output. While such an approach enables object-independent predictions, the downside is that it requires a long offline calibration procedure to obtain a large training dataset. Furthermore, the complexity of input images may limit the safety margin prediction frequency, which can be crucial for dynamic tasks.

To alleviate these issues, we propose an alternative approach, which is based on the identification of the relationship between the grip force F and the critical deformation δ^*. This identification approach can done manually online by the operator during the teleoperation and is further described in Section III-B. It should be noted that critical deformation δ^* is also dependent on object properties (e.g., surface material, etc.) and must be identified when dealing with a new object. To identify it, the operator can grasp an object with the remote gripper and increase the external load to induce a slippage. The deformations of the dots within the sensor show a peak when gross slip begins, which corresponds to the critical deformation. The critical deformation is collected for several different forces and fitted with a simple polynomial function that is used for autonomous online predictions by the robot.

Since detecting deformations with a vision-based sensor is difficult without a certain minimal pressure, we include a minimal grip force F_{min} in the controller as

$$F = \begin{cases} F_{min}, & \text{if } F < F_{min} \\ F, & \text{otherwise.} \end{cases} \tag{8}$$

D. Force Feedback

Force feedback informs the operator that contact is present when the remote gripper touches an object. This feedback activates during the initial moment of contact and consists of a short vibration of 0.5s at the local haptic interface

$$\theta_t = A \cdot sin(2\pi \cdot f \cdot t), \tag{9}$$

where A is the amplitude of the vibration, f is the frequency of the vibration, and t is the time. To determine if the gripper has contact with an object, the contact area of the gripper is monitored. When deformations in the contact area exceed a threshold, there is contact with an object. Once the deformations exceed the threshold, the position of the object surface x_{object} is stored. When the desired reference position, commanded by the operator, is greater than the position of the grasped object, $x_r > x_{object}$, contact is lost.

III. Experiments

We implemented the proposed adaptive semi-autonomous impedance controller on a teleoperation setup consisting of a local haptic device (Force Dimension Sigma.7) and a custom-built remote gripper mounted on a robotic arm (KUKA LBR iiwa7). The remote gripper was equipped with the ChromaTouch sensor to detect deformations for the safety margin (Section III-A). These different hardware systems were connected via a software interface based on Robot Operating System (ROS). Two proof-of-concept experiments are conducted to test the controller's functionalities (Section III-C). The first experiment, adaptability to external changes, demonstrates that the controller (autonomously) maintains grasp stability during load force changes. The second experiment, adaptability to human input, demonstrates the operator's control over the position of the remote gripper while holding an object.

A. Deformation tracking in the contact area

To detect deformations for the safety margin we employed the ChromaTouch sensor (Fig. 4), which was previously developed by our group [26], [27]. This sensor has a deformable dome in which two layers of coloured dots are present and are captured by a camera. When the sensor is

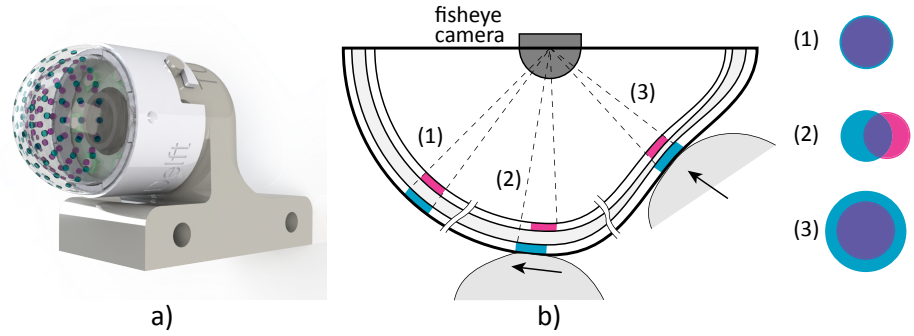

Fig. 4. a) The ChromaTouch sensor. b) The two-layered dotted dome of the sensor [27]: 1) deformations caused by indentation, 2) deformations caused by shear force, and 3) the dome during steady-state.

indented or a shear force is applied, the position, shape, and colour of the dots change. Deformations in the contact area are captured by tracking the changes in shape and position of the dots. We neglected the colour changes of the dots in this study as these are not of value during deformation detection.

The deformation was computed by tracking the position of the dots in the dome using OpenCV computer vision software (Fig. 5). In every image, 20 dots in the centre of the image are detected and labelled with the nearest neighbour algorithm. The labelled dots correspond to the same dot in the previous frame. Comparing the vertical position of the dots in different images give us the estimation of deformation. To reduce the noise in the position data caused by OpenCV, the average displacement of the 20 dots was placed into a moving time window of 10. The output of this window was the deformation δ in the contact area used in (7).

B. Critical deformation identification

Before conducting the experiments, we gathered data for the identification of critical deformation parameter δ^* with the proposed approach explained in Section II-C. The critical deformation δ^* is dependent on grip force F and object properties, therefore a dataset must be collected for a range of grip forces. To do so, the following protocol was used:

1) Grasp an object with the remote gripper, with a constant grip force.
2) Lift and hold the object in midair.
3) Add external load to the object until it shows displacement (gross slippage).
4) Record the deformation measured at the verge of slippage, which is the critical deformation.
5) Repeat this sequence for multiple grip forces and define a relation between the applied grip force and deformations.

For our experiments, the critical deformation is collected for seven different grip forces between 0 and 1.5 N.

C. Experimental protocol

1) Experiment 1: Adaptability to external changes: To demonstrate adaptability to external changes, an operator controlled the remote gripper and performed a pick-and-place task involving a metal can. While the object was held in midair, an extra load force was added to perturb the grasping

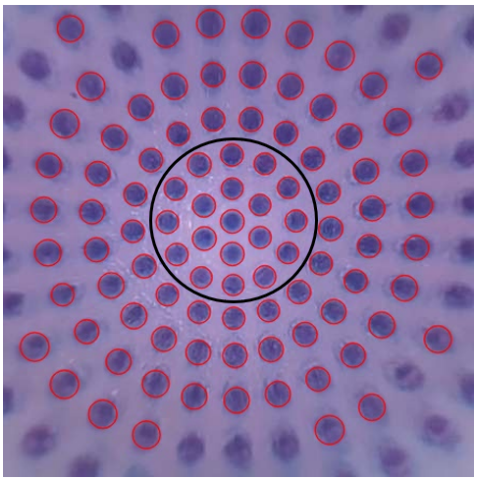

Fig. 5. Image of the inside of the ChromaTouch. The red circles are the detected dots with computer vision. The dots encircled by the black line are the 20 center dots tracked for the deformation.

action. To maintain grasp stability, the controller had to autonomously maintain the safety margin $Gamma$ around the reference margin $Gamma_r$ during different stages of the task. To do this, the controller had to change the grip force according to the load force by adapting the stiffness term based on sensory information. The task instructions followed these steps:

1) Close: position and close the remote gripper to grasp the object.
2) Lift and hold: lift the object with the remote gripper from the surface and hold it in midair at a specified position.
3) Add weight: hold the object (metal can) in midair while an extra weight (rice) is continuously poured into it.
4) Hold: hold the object in midair to show the grasp is stable.
5) Place and Open: place the object with the additional weight on the surface and open the gripper.

2) Experiment 2: Adaptability to human input: During the second experiment, the operator held the object in midair with the teleoperated remote gripper. While the object was held, the operator perturbed the reference position back and forth with an increasing magnitude for a while and then released it. When the commanded position was inside the

object, the controller had to adapt the stiffness term to maintain the reference safety margin $Gamma_r$ regardless of the commanded position changes x_r. When the commanded position x_r went outside of the object, the controller had to allow the operator to open the gripper and release the object. The task instructions followed these steps:

1) Hold object: hold the object in midair.
2) Gripper position perturbation: command variable desired gripper positions with increasing amplitude over time.
3) Gripper open: open the gripper to show the object can be released with the desired gripper position commands.

The parameter settings for the experiments are presented in Tab. I.

TABLE I

PARAMETERS FOR THE EXPERIMENTS

Defentition	Symbol	Value
Feed-forward value (initial stiffness)	K_0	20 [N/m]
Integral gain (stiffness adaptation module)	I	5 [N/(m·s)]
Reference grip force safety margin	Γ_r	30 [%]
Minimal grip force	F_{min}	0.6 [N]
Amplitude of feedback	A	1 [N]
Frequency of feedback	f	4 [Hz]

IV. RESULTS

A. Experiment 1: Adaptability to external changes

Fig. 6 shows the results of the proposed adaptive semi-autonomous adaptive impedance controller during external changes. In the first row of the graph, we can see that the operator initially closed the remote gripper and commanded the desired reference gripper position inside the object in order to grasp it. When the object was grasped the actual gripper position stopped following the commanded one as it remained on the object's surface.

The second row illustrates the safety margin, which was 0 when the gripper did not touch the object. Once the gripper was closed and the contact was established, the safety margin became 100% as there was no load force yet present (the object was still standing on the table). As the operator lifted the grasped object with the remote robot, the controller maintained the actual safety margin close to the desired safety margin of 30%. Furthermore, the controller maintained the desired safety margin when the load force increased after the additional unknown external load was added on top of the object. It is interesting to note that there was a slight noise in the safety margin signal, which could be related to the visual dot detection method that is used to compute the safety margin. However, the noise did not influence the task performance.

To maintain the reference safety margin of 30%, the semi-autonomous adaptive impedance controller adjusted its stiffness variable while the load force changed, as shown in the third column of the figure. The stiffness term increased to adapt the grip force to the increasing load force during the lifting phase of the object and the added unknown weight

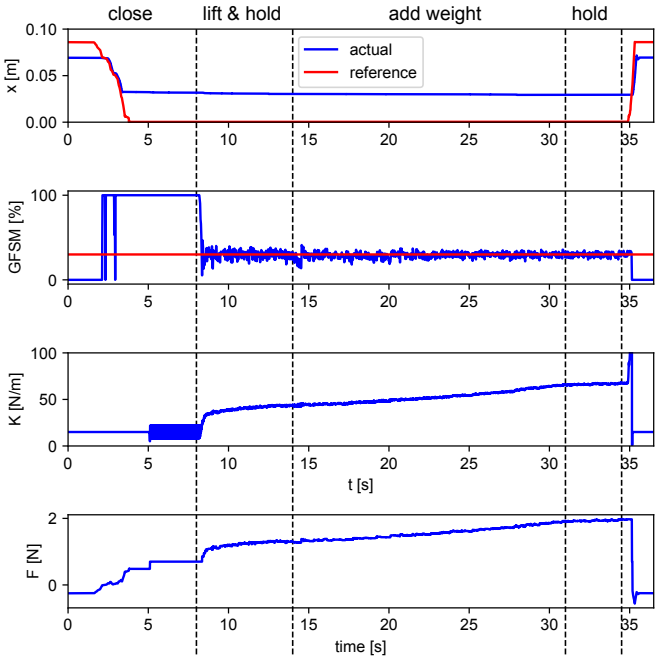

Fig. 6. Results of experiment 1: adaptability to external changes in load. The text on the top indicates the phases of the task during the experiment. The first graph shows the gripper aperture position. The second graph shows the grip force safety margin. The third graph shows gripper stiffness. The bottom graph shows the measured gripper force.

afterwards. The resulting grip force is illustrated in the last row where we can see how it adapted to accommodate the changes in the carried load.

Another particular behaviour in the stiffness term is present during $t = 5$s and $t = 8$s, where it fluctuates around 15 N/m. These fluctuations occur because the autonomous stiffness adaptation module tries to reduce the grip force as the actual safety margin is higher than desired. To reduce the grip force, the controller decreases the stiffness term. However, this is ineffective as the computed force is lower than the minimum required force. As a result, the minimal grip force is applied instead, according to (8). This fluctuation in the stiffness term did not cause undesired behaviour in the grip force and therefore did not influence the task performance.

B. Experiment 2: Adaptability to human input

Fig. 7 shows the results of the proposed semi-autonomous adaptive impedance controller's adaptability to human input regarding commanded gripper position. In the first graph, we can see the operator changing the desired gripper position while holding an object with the remote gripper. When the desired position was smaller than the actual position, i.e., the desired was inside the object, the remote gripper did not change the actual position since the object was grasped. When the desired position becomes larger than the actual, the actual position started to follow the desired position and the object was released.

We can see in the second graph that the controller maintained the desired safety margin of 30% while the remote

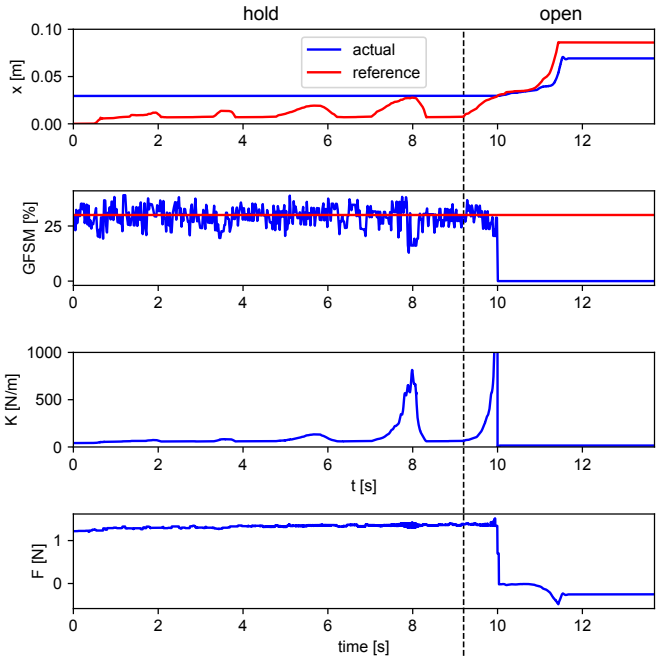

Fig. 7. Results of experiment 2: adaptability to human position commands. The text on the top indicates the phases of the task during the experiment. The first graph shows the gripper aperture position. The second graph shows the grip force safety margin. The third graph shows gripper stiffness. The bottom graph shows the measured gripper force.

gripper held the object. When the gripper opened, the safety margin naturally dropped to 0 as no object was held anymore.

The last two graphs display the stiffness and grip force, respectively. While the operator held the object, the controller applied a constant grip force to maintain the desired 30% safety margin, since there were no changes in the load. However, to maintain the needed grip force, the stiffness had to be adjusted to compensate for the changing difference between the desired and actual gripper position. As the difference in gripper position became smaller, the stiffness increased to maintain the constant grip force, as can be seen at $t = 4$s, $t = 6$s, and $t = 8$s.

V. Discussion

The purpose of this study was to develop a teleoperated control method which regulates the grip force autonomously to maintain grasp stability while the operator remains in control of the position of the remote gripper. To achieve this goal, we introduced the adaptive semi-autonomous impedance controller based on grip safety margin. We evaluated the semi-autonomous controller's functionalities by testing its adaptability to external changes and human input.

The results of the first experiment show that the semi-autonomous controller was able to maintain grasp stability during external perturbations. At the same time, the operator was able to control the position of the remote gripper, while the grip force is controlled autonomously by the robot to facilitate adaptation to the load changes. Compared to standard tele-impedance methods [15], the designed semi-autonomous feature offloads the operator of direct control of impedance. The key advantage is that the grasp stability is maintained by the robot without the need for the operator to constantly adjust the stiffness when the commanded position changes. Thus, the operator was able to perform the task even with very limited force feedback.

The results of the second experiment show that the controller can adapt to the human-commanded gripper position to maintain grasp stability. The controller achieved grasp stability by adapting the stiffness autonomously to regulate the grip force while the operator maintained the ability to open the gripper. Compared to a force controller, where the operator cannot control position as it is used to maintain constant desired force, the proposed adaptive semi-autonomous impedance controller enables the operator to have full control over the position of the gripper. At the same time, the designed adaptation of the grip force through stiffness based on the grip force safety margin maintains the advantages of the force controller regarding force regulation.

Compared to the state-of-the-art adaptive semi-autonomous impedance controllers [17]–[20], the proposed controller stands out by incorporating the safety margin to maintain grasp stability autonomously. This feature enables it to prevent slippage during task perturbations by proactively regulating the grip force. Consequently, the operator does not need to manually react to these rapid changes. However, to do so, our controller requires critical displacement parameters to achieve grasp stability. Since the critical displacement is dependent on a specific object, we must be able to detect what object is being grasped and have a dataset of appropriate critical displacements. Thus, an extra sensory system is required.

A potential future work would be to develop object-independent safety margin detection to reduce the dependency on critical deformation. Machine learning can be employed to compute the safety margin without prior known object properties [28]. However, a downside of the machine learning approach is the need for a large amount of training data. Another potential future work direction is to solve the limitation related to ChromaTouch sensor. As the sensor dome is stiff, displacements of the dots only occur when a certain applied force threshold is exceeded (hence (8) was needed). This can become problematic when grasping very delicate objects and decreasing this threshold would improve the sensitivity of the approach. A further improvement could be made by replacing the simple vibrational feedback (as described in Section II-D) with more complex tactile feedback if the operator wants to switch to full control over grasping.

The evaluation of the proposed method in this study was limited to proof-of-concept experiments. In future, the method evaluation should go beyond proof-of-concept experiments, which could involve tasks beyond pick-and-place and other objects.

Acknowledgements

The authors would like to thank Dirk-Jan Boonstra and Laurence Willemet for their assistance with the experiment setup.

REFERENCES

[1] K. Kaneko, M. Morisawa, S. Kajita, S. Nakaoka, T. Sakaguchi, R. Cisneros, and F. Kanehiro, "Humanoid robot HRP-2Kai - improvement of HRP-2 towards disaster response tasks," in *2015 IEEE-RAS 15th International Conference on Humanoid Robots (Humanoids)*. IEEE, 2015, pp. 132–139.

[2] K. J. Cole and R. S. Johansson, "Friction at the digit-object interface scales the sensorimotor transformation for grip responses to pulling loads," *Experimental Brain Research*, vol. 95, pp. 523–532, 1993.

[3] T. Zackrisson, B. Eriksson, N. Hosseini, B. Johnels, and A.-L. Krogstad, "Patients with hyperhidrosis have changed grip force, coefficient of friction and safety margin," *Acta neurologica scandinavica*, vol. 117, no. 4, pp. 279–284, 2008.

[4] R. S. Johansson and J. R. Flanagan, "Coding and use of tactile signals from the fingertips in object manipulation tasks," *Nature Reviews Neuroscience*, vol. 10, no. 5, pp. 345–359, 2009.

[5] M. Santello, M. Flanders, and J. F. Soechting, "Patterns of hand motion during grasping and the influence of sensory guidance," *Journal of Neuroscience*, vol. 22, no. 4, pp. 1426–1435, 2002.

[6] Z. Lu, L. Chen, H. Dai, H. Li, Z. Zhao, B. Zheng, N. F. Lepora, and C. Yang, "Visual-tactile robot grasping based on human skill learning from demonstrations using a wearable parallel hand exoskeleton," *IEEE Robotics and Automation Letters*, vol. 8, no. 9, pp. 5384–5391, 2023.

[7] E. D. Engeberg and S. G. Meek, "Adaptive sliding mode control for prosthetic hands to simultaneously prevent slip and minimize deformation of grasped objects," *IEEE/ASME Transactions on Mechatronics*, vol. 18, no. 1, pp. 376–385, 2011.

[8] F. Cordella, C. Gentile, L. Zollo, R. Barone, R. Sacchetti, A. Davalli, B. Siciliano, and E. Guglielmelli, "A force-and-slippage control strategy for a poliarticulated prosthetic hand," in *2016 IEEE International Conference on Robotics and Automation (ICRA)*. IEEE, 2016, pp. 3524–3529.

[9] C. Gentile, G. Lunghi, L. R. Buonocore, F. Cordella, M. Di Castro, A. Masi, and L. Zollo, "Manipulation tasks in hazardous environments using a teleoperated robot: A case study at cern," *Sensors*, vol. 23, no. 4, p. 1979, 2023.

[10] J. Zhang, D. Xu, Z.-T. Zhang, and W.-S. Zhang, "Position/force hybrid control system for high precision aligning of small gripper to ring object," *International Journal of Automation and Computing*, vol. 10, no. 4, pp. 360–367, 2013.

[11] A. Ajoudani, S. B. Godfrey, M. Bianchi, M. G. Catalano, G. Grioli, N. Tsagarakis, and A. Bicchi, "Exploring teleimpedance and tactile feedback for intuitive control of the pisa/iit softhand," *IEEE transactions on haptics*, vol. 7, no. 2, pp. 203–215, 2014.

[12] V. R. Garate, M. Pozzi, D. Prattichizzo, N. Tsagarakis, and A. Ajoudani, "Grasp stiffness control in robotic hands through coordinated optimization of pose and joint stiffness," *IEEE Robotics and Automation Letters*, vol. 3, no. 4, pp. 3952–3959, 2018.

[13] J. P. Clark, G. Lentini, F. Barontini, M. G. Catalano, M. Bianchi, and M. K. OMalley, "On the role of wearable haptics for force feedback in teleimpedance control for dual-arm robotic teleoperation," in *2019 International Conference on Robotics and Automation (ICRA)*. IEEE, 2019, pp. 5187–5193.

[14] E. Hocaoglu and V. Patoglu, "semg-based natural control interface for a variable stiffness transradial hand prosthesis," *Frontiers in Neurorobotics*, vol. 16, 2022.

[15] L. Peternel and A. Ajoudani, "After a decade of teleimpedance: A survey," *IEEE Transactions on Human-Machine Systems*, vol. 53, no. 2, pp. 401–416, 2022.

[16] L. Peternel, N. Beckers, and D. A. Abbink, "Independently commanding size, shape and orientation of robot endpoint stiffness in teleimpedance by virtual ellipsoid interface," in *2021 20th International Conference on Advanced Robotics (ICAR)*. IEEE, 2021, pp. 99–106.

[17] A. Brygo, I. Sarakoglou, N. Tsagarakis, and D. G. Caldwell, "Tele-manipulation with a humanoid robot under autonomous joint impedance regulation and vibrotactile balancing feedback," in *2014 IEEE-RAS International Conference on Humanoid Robots*. IEEE, 2014, pp. 862–867.

[18] L. Muratore, A. Laurenzi, E. M. Hoffman, L. Baccelliere, N. Kashiri, D. G. Caldwell, and N. G. Tsagarakis, "Enhanced tele-interaction in unknown environments using semi-autonomous motion and impedance regulation principles," in *2018 IEEE International Conference on Robotics and Automation (ICRA)*. IEEE, 2018, pp. 5813–5820.

[19] Y.-C. Huang, D. A. Abbink, and L. Peternel, "A semi-autonomous tele-impedance method based on vision and voice interfaces," in *2021 20th International Conference on Advanced Robotics (ICAR)*. IEEE, 2021, pp. 180–186.

[20] C. Zeng, S. Li, Z. Chen, C. Yang, F. Sun, and J. Zhang, "Multifingered robot hand compliant manipulation based on vision-based demonstration and adaptive force control," *IEEE Transactions on Neural Networks and Learning Systems*, 2022.

[21] N. Hogan, "Impedance control: An approach to manipulation," *Journal of dynamic systems, measurement, and control*, vol. 107, no. 1, pp. 1–24, 1985.

[22] A. Albu-Schaffer, C. Ott, U. Frese, and G. Hirzinger, "Cartesian impedance control of redundant robots: Recent results with the dlr-light-weight-arms," in *2003 IEEE International Conference on Robotics and Automation (ICRA)*. IEEE, 2003, pp. 3704–3709.

[23] L. Willemet, N. Huloux, and M. Wiertlewski, "Efficient tactile encoding of object slippage," *Scientific Reports*, vol. 12, no. 1, p. 13192, 2022.

[24] S. Teshigawara, T. Tsutsumi, S. Shimizu, Y. Suzuki, A. Ming, M. Ishikawa, and M. Shimojo, "Highly sensitive sensor for detection of initial slip and its application in a multi-fingered robot hand," in *2011 IEEE International Conference on Robotics and Automation (ICRA)*. IEEE, 2011, pp. 1097–1102.

[25] J. Reinecke, A. Dietrich, F. Schmidt, and M. Chalon, "Experimental comparison of slip detection strategies by tactile sensing with the biotac® on the dlr hand arm system," in *2014 IEEE international Conference on Robotics and Automation (ICRA)*. IEEE, 2014, pp. 2742–2748.

[26] X. Lin and M. Wiertlewski, "Sensing the frictional state of a robotic skin via subtractive color mixing," *IEEE Robotics and Automation Letters*, vol. 4, no. 3, pp. 2386–2392, 2019.

[27] R. B. Scharff, D.-J. Boonstra, L. Willemet, X. Lin, and M. Wiertlewski, "Rapid manufacturing of color-based hemispherical soft tactile fingertips," in *2022 IEEE 5th International Conference on Soft Robotics (RoboSoft)*. IEEE, 2022, pp. 896–902.

[28] D. Boonstra, "Learning to estimate the proximity of slip using high-resolution tactile sensing," *Master Thesis*, 2022.